

Kardar-Parisi-Zhang fluctuations in the synchronization dynamics of limit-cycle oscillators

Ricardo Gutiérrez¹ and Rodolfo Cuerno¹

¹*Grupo Interdisciplinar de Sistemas Complejos (GISC), Departamento de Matemáticas, Universidad Carlos III de Madrid, 28911 Leganés, Madrid, Spain*

The space-time process whereby one-dimensional systems of self-sustained oscillators synchronize is shown to display generic scale invariance, with scaling properties characteristic of the Kardar-Parisi-Zhang equation with columnar noise, and phase fluctuations that follow a Tracy-Widom probability distribution. This is revealed by a numerical exploration of rings of Stuart-Landau oscillators (the universal representation of an oscillating system close to a Hopf bifurcation) and rings of van der Pol oscillators, both of which are paradigms of self-sustained oscillators. The critical behavior is very well-defined for limit-cycle oscillations near the bifurcation point, and still dominates the behavior comparatively far from the bifurcation. In particular, the Tracy-Widom fluctuation distribution seems to be an extremely robust feature of the synchronization process. The nonequilibrium criticality here described appears to transcend the details of the coupled dynamical systems that synchronize, making plausible its experimental observation.

A great variety of natural and technological systems comprising several dynamical units exhibit, and sometimes crucially rely on, synchronous dynamics [1]. The list includes ensembles of neurons and heart cells, fireflights, flocking birds and humans, coupled pendula and quantum oscillators. They may be theoretically described as few- or many-body systems of oscillators, with regular or chaotic dynamics, subjected to external forcing or mutual coupling, with all-to-all, periodic, or irregular interaction patterns. All such cases present synchronization and have been intensively researched [2–4].

Key properties of the time-dependent process whereby spatially-coupled oscillators reach synchronization can be elucidated through the theoretical framework of surface kinetic roughening [5–7], employed in the study of nonequilibrium growth processes like the formation of e.g. thin solid films, bacterial colonies, or coffee rings. Such framework is lately proving to be of a broader relevance, as it accounts for the behavior of non-interfacial systems also, from the evolution of Lyapunov vectors in space-time chaos [8–11] to one-dimensional (1D) dynamics of fermions and bosons [12–14], or to the kinetics of chemical reactions [15]. Indeed, all these systems display universal behavior akin to equilibrium critical dynamics [16, 17], without parameter fine tuning to precise critical values, providing instances of generic scale invariance (GSI) [18–20]. The Kardar-Parisi-Zhang (KPZ) equation [21–23] is paramount in this context, as its universality class applies to the critical behavior of fluctuations in many low-dimensional, strongly correlated systems, from surface growth processes [5–7] to novel contexts like active [24] or quantum [25, 26] matter. Recently, the ubiquity of KPZ universality seems connected to the fact the statistics of fluctuations in those systems are governed [22, 23] by the (non-Gaussian) Tracy-Widom (TW) family of probability density functions (PDF) for random matrix eigenvalues [27, 28], found across length scales in an astounding variety of systems [29].

In the synchronization context, a formal connection with the main equations of surface kinetic roughening has been pointed out repeatedly in the literature [1, 2, 30–33]. For *idealized oscillators*, we have elucidated this connection [34], showing that the synchronization process in a lattice of such systems displays GSI and specific forms of kinetic-roughening universality. Namely, for odd-symmetric coupling functions, such as the sine function of the celebrated Kuramoto model [35], the KPZ nonlinearity plays no role [34], and the resulting effective description is the (linear) Edwards-Wilkinson equation with columnar quenched disorder, also known as the Larkin model [36], featuring Gaussian fluctuations. Otherwise, for generic coupling functions, all terms of the KPZ equation are at play, inducing the universality class of the columnar KPZ equation [37], with TW fluctuations [34]. These results depend on two strong assumptions, however: I) the dynamical units are phase oscillators (i.e. idealized self-sustained oscillators), and II) the coupling function among them is purely sinusoidal.

In this Letter, we elucidate the universal features of the synchronization process in lattices of full-fledged, self-sustained oscillators of the Stuart-Landau (SL) and van der Pol (vdP) types. While the SL model is a canonical representation of an oscillating system close to its Hopf bifurcation [2], the vdP model is a paradigmatic system of experimental relevance [1, 38]. We thus bypass the limitations of Ref. [34] by studying generic limit-cycle oscillators, with coupling functions that are not necessarily sinusoidal at the phase-reduced level [39, 40]. To do so, we adapt the observables and analyses employed to assess universal behavior in kinetic roughening to the study of the phase dynamics [1] of coupled SL or vdP oscillators, the phases themselves playing a role analogous to that of local heights in interfacial systems [5–7]. Intuitively, a “phase interface” grows above a “substrate” of oscillators, an analogy fruitfully explored in various recent works dealing with phase oscillators [34, 41, 42]; see

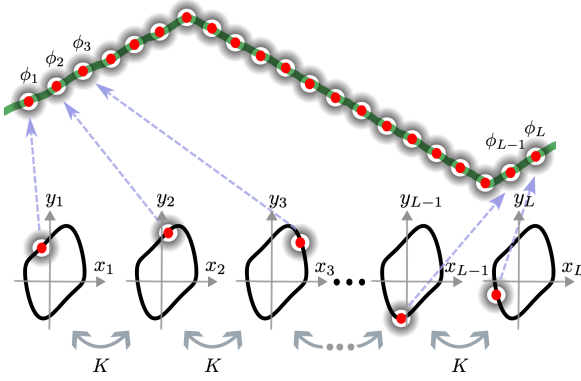


FIG. 1. Phases $\phi_j(t)$ extracted from the states of oscillators form an “interface” above an oscillator “substrate”, where the subindex j identifies an oscillator by its position along the lattice. The limit cycle shown is for a single vdP oscillator with $\mu = 1$, Eq. (7), $K = 0$, and the green interface is a snapshot of simulations of the same equation for $K \neq 0$.

Fig. 1 for an illustration. Our results show that GSI is robust for the synchronization process, and generically corresponds to the universality class of the columnar KPZ equation, with TW-distributed fluctuations, as for idealized phase oscillators with non-odd coupling [34]. This makes plausible the experimental observation of such nonequilibrium criticality in synchronous dynamics.

Stuart-Landau oscillators—A SL oscillator is the normal form of a nonlinear dynamical system undergoing a supercritical Hopf bifurcation, where a fixed point loses stability and a small-amplitude limit cycle branches from it [43, 44]. We consider a 1D chain of L such oscillators with periodic boundary conditions (PBC, i.e. a ring), namely,

$$\dot{z}_j(t) = a_j z_j(t) - b_j |z_j(t)|^2 z_j(t) + K c_j [z_{j+1}(t) + z_{j-1}(t) - 2z_j(t)], \quad (1)$$

where a dot denotes time derivative and $j = 1, 2, \dots, L$. The j -th oscillator is described by the complex-valued function $z_j(t)$, while $a_j = \mu + i\omega_j$, $b_j = 1$, $c_j = 1 + i \in \mathbb{C}$, and the coupling strength $K \in \mathbb{R}$, are constants. Here, μ measures the distance to the ($\mu_c = 0$) bifurcation point, and the intrinsic frequency ω_j is oscillator-dependent. The first line on the right-hand side of Eq. (S1) contains the standard SL-oscillator dynamics [44], and the second line adds a (diffusive) nearest-neighbor coupling, where $z_0(t) \equiv z_L(t)$ and $z_{L+1}(t) \equiv z_1(t)$.

In the uncoupled case ($K = 0$), each oscillator has a circular stable limit cycle on the complex plane given by $z_j(t) = R_j(t) \exp\{i\theta_j(t)\}$, with radius $R_j(t) = \sqrt{\mu}$ and geometric phase $\theta_j(t) = \omega_j t$ [44], the latter being a valid dynamical phase variable [1]. Outside the limit cycle (for $R_j(t) \neq \sqrt{\mu}$), an asymptotic phase [2] can be explicitly defined as $\phi(z_j(t)) = \theta_j(t)$ (i.e. the dynamic phase is the geometric phase everywhere in phase space), which provides a set of isochrones covering phase space, such that on each one of them $\dot{\phi}(z_j(t)) = \omega_j$ [43]. One can

thus easily extract the instantaneous phases $\{\phi_j(t)\}_{j=1}^L$ from the states $\{z_j(t)\}_{j=1}^L$ (on or off the limit cycle) of the oscillators whose dynamics are governed by Eq. (S1).

In our simulations, the intrinsic frequencies ω_j are chosen at random from a uniform distribution on an interval of width ϵ centered around 1, i.e. $\omega_j \sim U([1 - \epsilon/2, 1 + \epsilon/2])$. The ensuing heterogeneity is akin to that found in phase-oscillator models like the Kuramoto model [35]. In the kinetic roughening literature [6] this is known as *columnar noise*, i.e. quenched disorder that only depends on the substrate position (oscillator), not on the height (phase) value. In practice, we take $\epsilon = 0.1$, while we inspect various values of μ , which also determines the coupling strength, $K = \mu$. The equation set (S1) is integrated by a 4-th order Runge-Kutta method with step size 0.01—to be employed for our vdP oscillators too—from the initial condition $z_j(0) = \sqrt{\mu}$ for all j .

The deviations of the local phases around their mean value are measured by the global width or roughness,

$$W(L, t) \equiv \overline{\langle [\phi(x, t) - \overline{\phi(x, t)}]^2 \rangle}^{1/2}, \quad (2)$$

with the overbar denoting spatial average in a substrate of size L and the brackets denoting average over different noise realizations, as is standard for kinetically rough interfaces [5]. Here W saturates if the phase differences remain bounded in time, which only happens when all oscillators reach a common effective frequency. Thus, saturation manifests synchronization (i.e. frequency entrainment) [34], only occurring for coupling strengths K above the threshold value K_c . In surface kinetic roughening, the heights (here, the phases) are statistically correlated for distances below a correlation length $\xi(t)$ increasing with time as $\xi(t) \sim t^{1/z}$, where z is the so-called dynamic exponent. This behavior holds until $\xi(t)$ reaches a value comparable to $L \gg 1$, implying saturation of the width at a steady-state, size-dependent value $W(L, t \gg L^z) \sim L^\alpha$, where the roughness exponent α characterizes the fractality of the phase profile $\{\phi_j(t)\}_{j=1}^L$. Prior to saturation, the roughness increases in time as $W(t) \sim t^\beta$, where $\beta = \alpha/z$ [5–7].

In Fig. 2(a) we show the roughness $W(L, t)$ for systems of $L = 500$ and 1000 SL oscillators. For each L , we consider two different values $\mu = 0.5$ and 2, both of which yield $K = \mu > K_c$, so that synchronization is achieved, which as expected occurs later for larger systems. Before saturation, a growth regime is observed in which $W \sim t^\beta$ closely, for $\beta \approx 0.78$. This corresponds to the choice of exponent values $\alpha = 1.07$ and $z = 1.37$, justified below.

Beyond the roughness, kinetic roughening also manifests itself in the space-time behavior of correlation functions [5–7]. A very useful one [45, 46] is the power spectral density of phase fluctuations,

$$S(k, t) \equiv \langle \hat{\phi}(k, t) \hat{\phi}(-k, t) \rangle = \langle |\hat{\phi}(k, t)|^2 \rangle, \quad (3)$$

where $\hat{\phi}(k, t)$ is the (1D) space Fourier transform of $\phi_j(t)$

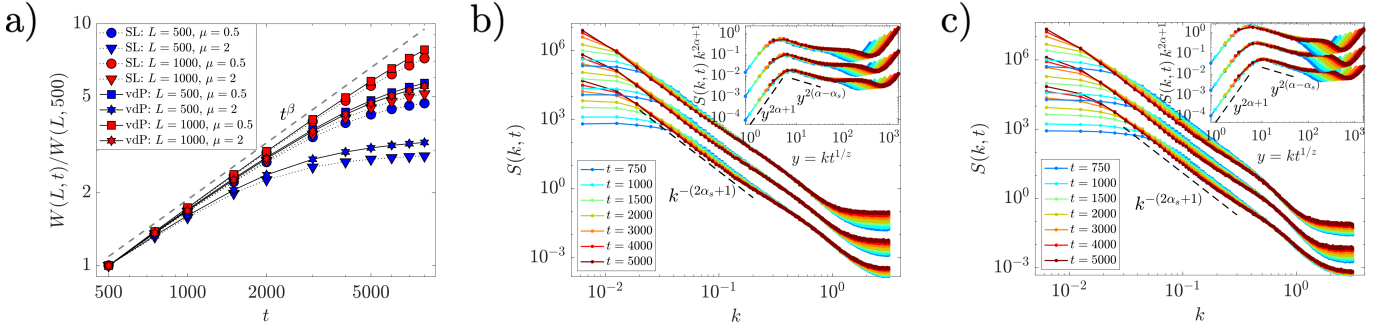


FIG. 2. (a) Roughness normalized with respect to its value at $t = 500$, $W(L, t)/W(L, 500)$, as a function of time for different sizes L in rings of SL oscillators and rings of vdp oscillators. Two choices of the parameter μ are displayed (see legend). The dashed line represents a power-law growth t^β . Panels (b) and (c): Structure factor $S(k, t)$ at times as in the legend, for rings of $L = 1000$ SL oscillators [(b), main panel] and of vdp oscillators [(c), main panel]. In both panels the insets show the rescaling of the $S(k, t)$ data of the main panel following Eq. (4). Results are for $\mu = 0.5, 1$, and 2.0 , the last two values shown after an upward vertical displacement, so that larger values of μ appear above, for visibility purposes. In all three panels, the exponent values used are $\alpha = 1.07$, $z = 1.37$, and $\alpha_s = 1.40$ ($\beta = \alpha/z \approx 0.78$). Results based on 1000 realizations.

and k is wavenumber. As a generalization of equilibrium critical behavior [17], in kinetic roughening this correlation function satisfies the scaling form [47]

$$S(k, t) = k^{-(2\alpha+1)} s(kt^{1/z}), \quad (4)$$

where the scaling function $s(y) \propto y^{2(\alpha-\alpha_s)}$ for $y \gg 1$ and $s(y) \propto y^{2\alpha+1}$ for $y \ll 1$. Here, an additional (spectral roughness) exponent α_s appears, which characterizes length scales smaller than $\xi(t)$, as Eq. (4) implies that $S(k, t) \sim 1/k^{2\alpha_s+1}$ for $k \gg 1/t^{1/z}$. In the simplest cases, as for the KPZ equation with time-dependent noise, $\alpha_s = \alpha$ and Eq. (4) reduces to the celebrated Family-Viscsek dynamic scaling Ansatz [5–7, 48]. However, in our case $\alpha_s \neq \alpha$ are independent exponents such that $\alpha_s, \alpha > 1$, a behavior known as faceted anomalous scaling [47]. Indeed, Fig. S2 in the Supplemental Material (SM) [40] illustrates the formation of triangular facets in the phase “interface” $\phi_j(t)$ along the evolution corresponding to Fig. 2(b). The latter figure shows the structure factor in a ring of $L = 1000$ SL oscillators, for $\mu = 0.5, 1$, and 2 . An upward vertical displacement, larger for higher μ , has been applied to the last two values to ease visualization. The main panel shows $S(k, t)$ as a function of k for several times, while the inset shows the same data in rescaled form according to Eq. (4), with $\alpha = 1.07$, $z = 1.37$, and $\alpha_s = 1.40 \neq \alpha$ [49]. The data collapse is very good except for wavenumbers close to the discretization cutoff. A peculiar implication of these exponent values is that two-point correlations (related with $S(k, t)$ via Fourier transforms [7]) scale with a different roughness exponent in real space [7, 47, 50–53]. E.g., by defining $G(r, t) = \langle (\phi_{j+r}(t) - \phi_j(t))^2 \rangle$, under faceted anomalous scaling [47] $G(r) \sim r^{2\alpha_{\text{loc}}}$, where $\alpha_{\text{loc}} = 1 \neq \alpha \neq \alpha_s$. For the simulations in Figs. 2(a)–(b), $\alpha_{\text{loc}} = 0.97$ (see the SM [40]), the difference with the expected value possibly being a finite-size effect.

As recently highlighted for e.g. KPZ-related systems [22, 23], the statistics of phase fluctuations $\phi_j(t)$ around their mean $\bar{\phi}(t)$ is another trait of a kinetic roughening universality class. We thus study the PDF of

$$\varphi_j \equiv \frac{\delta\phi_j(t_0 + \Delta t) - \delta\phi_j(t_0)}{(\Delta t)^\beta}, \quad (5)$$

where $j = 1, 2, \dots, L$ and $\delta\phi_j(t) = \phi_j(t) - \bar{\phi}(t)$; t_0 is a reference time beyond the initial transient dynamics, and $t_0 + \Delta t$ is an intermediate time within the growth regime. The division by $(\Delta t)^\beta$ removes the systematic increase of the fluctuations in time so that, remarkably, the PDF of φ_j reaches a universal, time-independent form [22, 23]. Examples in the kinetic roughening context are the Gaussian distribution for the linear EW equation [5, 7] and a TW PDF (depending, e.g., on boundary conditions) for the KPZ equation [22, 23]. In lattices of phase oscillators, the former is observed for Kuramoto coupling and the latter for generic coupling functions [34]. For rings of SL oscillators, Fig. 3 shows the histograms of fluctuations φ_j for $\mu = 0.5, 1$, and 2 . Specifically, the main panel allows to inspect the tails of the distribution, while the top-left inset shows the values around the peak. Data follow quite closely the Gaussian Orthogonal Ensemble (GOE)-TW PDF, as for the 1D KPZ equation with time-dependent noise and PBC [22, 23].

Finally, two-point fluctuation statistics are also universal and can be assessed [23] through the phase covariances

$$C(r, t) \equiv \overline{\langle \phi_j(t) \phi_{j+r}(t) \rangle} - \langle \bar{\phi}(t) \rangle^2. \quad (6)$$

They are shown in the bottom-center inset of Fig. 3 for the same three values of μ . In the growth regime [22, 23], $C(\ell, t) = a_1 t^{2\beta} \mathcal{C}(a_2 \ell/t^{1/z})$, where \mathcal{C} is a scaling function, $\ell \equiv |r|$, and a_1 and a_2 are constants. To fix them [54], we have chosen the covariance of the Airy₁ process, which

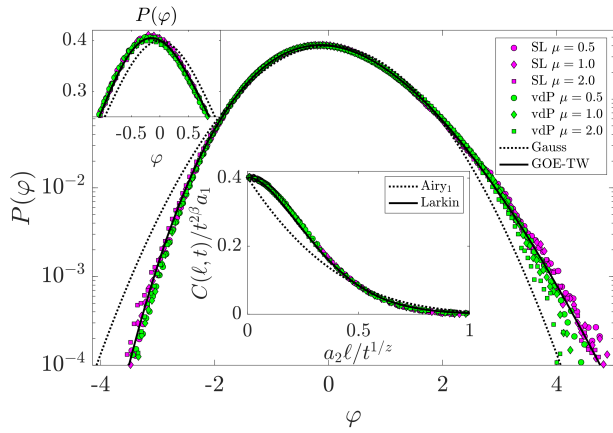


FIG. 3. (Main panel) Histogram of phase fluctuations, Eq. (5), in rings of $L = 1000$ SL oscillators and vdP oscillators for $\mu = 0.5, 1$, and 2 . (Top-left inset) Same data in linear scale, centered around the peak of the distribution. The dotted (solid) line represents a Gaussian (GOE-TW) PDF. Data for the histograms are based on 10000 realizations, for $t = 300, 500, 700, 1000, 1500$, and 2000 ($t_0 = 100$, and $\Delta t = 200, 400, \dots, 1900$), in the growth regime. (Bottom-center inset) Rescaled phase covariance, Eq. (6), for rings of SL and vdP oscillators with parameter values as in (a), for $t = 500, 550, 600, \dots, 800$. The dotted (solid) line represents the covariance of the Airy₁ process (Larkin model). The exponent values are $\alpha = 1.07$ and $z = 1.37$ ($\beta = \alpha/z \approx 0.78$).

occurs in the 1D KPZ class with PBC [23] and appears as a black dotted line, as the functional form for $\mathcal{C}(x)$. Instead, the results follow quite closely the covariance of the Larkin model [34, 36]. Figure 3 for the SL rings thus agrees with the fluctuation PDF and phase covariance that we have recently found [34] for phase oscillators with a generic (non-odd) sinusoidal coupling function, as analytically implied by a phase reduction study, see the SM [40]. Still, the occurrence of such PDF and covariance is far from trivial, as the coupling between the oscillators is relatively strong, the differences in their intrinsic frequencies are sizeable, and the distance to the bifurcation point is considerable, while phase-reduction techniques work best for almost identical weakly-coupled oscillators close to the bifurcation [39]. For a still more radical departure from idealized regimes, we next study a physically-motivated oscillator which behaves very differently far from its bifurcation threshold.

van der Pol oscillators— The vdP oscillator has played a central role in the development of nonlinear science [1, 38, 55]. We analyze a ring of L coupled oscillators (generalizing the $L = 2$ case [56]), whose evolution reads

$$\ddot{x}_j = (\mu - x_j^2) \dot{x}_j - \omega_j^2 x_j + K[(x_{j+1} + x_{j-1} - 2x_j) + (\dot{x}_{j+1} + \dot{x}_{j-1} - 2\dot{x}_j)], \quad (7)$$

where $j = 1, 2, \dots, L$. The state of the j -th oscillator is given by the pair of real numbers $(x_j(t), \dot{x}_j(t))$, with $x_0(t) \equiv x_L(t)$ and $x_{L+1}(t) \equiv x_1(t)$. The first two terms

on the right-hand side are those of the vdP oscillator, the remaining one being a diffusive coupling term with strength K . In the absence of coupling ($K = 0$), the j -th dynamical unit oscillates with amplitude proportional to $\sqrt{\mu}$ at an intrinsic frequency ω_j for $\mu > 0$. The critical value $\mu_c = 0$ is the bifurcation point of a supercritical Hopf bifurcation [38]. We explore different values of $K = \mu > K_c > 0$, so that synchronization occurs in all cases. The intrinsic frequencies ω_j are again random, taken from a uniform distribution, $\omega_j \sim U([0.95, 1.05])$.

For sufficiently small μ one might expect a similar behavior to that found for our SL oscillators, Eq. (S1). As μ is increased, however, the vdP oscillator behaves more as a relaxation oscillator, moving across different regions of the limit cycle (which differs from a circle, see Fig. 1 for $\mu = 1$) at different speeds [38]. Thus, the geometric $\arctan(\dot{x}_j/x_j)$ phase no longer behaves as a valid dynamical phase variable [1] and the phase $\phi_j(t)$ is instead defined by a Poincaré section [1], see the SM [40] for details.

In Fig. 2(a) we show the roughness $W(L, t)$ for rings of vdP oscillators in which $\mu = 0.5$ and 2 , ranging from close to μ_c , well into relaxation oscillation values of μ . Figure 2(c) displays the structure factor $S(k, t)$ across time, vertically shifted as in Fig. 2(b). These data are collapsed in the inset, according to Eq. (4), using the same exponent values as for the SL oscillators. Again, collapse is very good except for k values close to the discretization cutoff.

In Fig. 3(main panel and top-left inset), the distribution of fluctuations φ_j in the system of vdP oscillators is shown to follow quite closely the GOE-TW PDF, as for SL oscillators. This might be expected close to bifurcation ($\mu \ll 1$), as the phase reduction is expected to be accurate there, and the coupling function of the phase oscillators is not an odd function (which would imply Gaussian fluctuations [34]), see the SM [40]. Actually, we find that the GOE-TW fluctuation PDF is a robust feature of synchronization that holds even for large μ . The same can be said about the phase covariance $\mathcal{C}(r, t)$, shown in Fig. 3(bottom-center inset), which again closely follows the covariance of the Larkin model [34].

Conclusions— Overall, for the two paradigmatic 1D systems of self-sustained oscillators that we study, synchronization emerges in time displaying GSI compatible with the faceted scaling of the columnar KPZ equation, a TW PDF, and a Larkin covariance. The same critical behavior was recently observed for idealized phase oscillators with harmonic couplings [34]. The columnar KPZ equation is known to be prone to nonuniversal corrections [7, 37, 57, 58] arising, in our case, from changes in the intrinsic frequency distribution, which may justify the small differences in the critical exponent values we obtain with respect to those reported in Ref. [37]. Still, the behavior we observe is robust and occurs even far from the bifurcation. Given the experimental relevance of e.g. vdP oscillators [1, 55, 59, 60], our results make the observation of such nonequilibrium criticality,

e.g. for coupled nonlinear electronic circuits or oscillating chemically-reacting media, an alluring possibility.

Acknowledgements— This work has been partially supported by Ministerio de Ciencia e Innovación (Spain), by Agencia Estatal de Investigación (AEI, Spain, 10.13039/501100011033), and by European Regional Development Fund (ERDF, A way of making Europe) through Grants No. PID2021-123969NB-I00 and No. PID2021-128970OA-I00, and by Comunidad de Madrid (Spain) under the Multiannual Agreement with UC3M in the line of Excellence of University Professors (EPUC3M23), in the context of the V Plan Regional de Investigación Científica e Innovación Tecnológica (PRICIT).

-
- [1] A. Pikovsky, M. Rosenblum, and J. Kurths, *Synchronization: A Universal Concept in Nonlinear Sciences* (Cambridge University Press, Cambridge, UK, 2001).
 - [2] Y. Kuramoto, *Chemical Oscillations, Waves, and Turbulence* (Springer, Berlin, 1984).
 - [3] S. Boccaletti, J. Kurths, G. Osipov, D.L. Valladares, and C.S. Zhou, “The synchronization of chaotic systems,” *Phys. Rep.* **366**, 1 (2002).
 - [4] A. Arenas, A. Díaz-Guilera, J. Kurths, Y. Moreno, and C. Zhou, “Synchronization in complex networks,” *Phys. Rep.* **469**, 93 (2008).
 - [5] A.-L. Barabási and H. E. Stanley, *Fractal Concepts in Surface Growth* (Cambridge University Press, Cambridge, UK, 1995).
 - [6] T. Halpin-Healy and Y. C. Zhang, “Kinetic roughening phenomena, stochastic growth, directed polymers and all that. Aspects of multidisciplinary statistical mechanics,” *Phys. Rep.* **254**, 215 (1995).
 - [7] J. Krug, “Origins of scale invariance in growth processes,” *Adv. Phys.* **46**, 139 (1997).
 - [8] A. S. Pikovsky and J. Kurths, “Roughening interfaces in the dynamics of perturbations of spatiotemporal chaos,” *Phys. Rev. E* **49**, 898 (1994).
 - [9] A. Pikovsky and A. Politi, “Dynamic localization of Lyapunov vectors in spacetime chaos,” *Nonlinearity* **11**, 1049 (1998).
 - [10] D. Pazó and J. M. López, “Characteristic Lyapunov vectors in chaotic time-delayed systems,” *Phys. Rev. E* **82**, 056201 (2010).
 - [11] Y. T. Fukai and K. A. Takeuchi, “Initial perturbation matters: Implications of geometry-dependent universal Kardar–Parisi–Zhang statistics for spatiotemporal chaos,” *Chaos* **31** (2021).
 - [12] K. Fujimoto, R. Hamazaki, and Y. Kawaguchi, “Family-Vicsek Scaling of Roughness Growth in a Strongly Interacting Bose Gas,” *Phys. Rev. Lett.* **124**, 210604 (2020).
 - [13] K. Fujimoto, R. Hamazaki, and Y. Kawaguchi, “Dynamical Scaling of Surface Roughness and Entanglement Entropy in Disordered Fermion Models,” *Phys. Rev. Lett.* **127**, 090601 (2021).
 - [14] K. Fujimoto, R. Hamazaki, and Y. Kawaguchi, “Impact of Dissipation on Universal Fluctuation Dynamics in Open Quantum Systems,” *Phys. Rev. Lett.* **129**, 110403 (2022).
 - [15] S. Mondal, J. S. Greenberg, and J. R. Green, “Universal dynamic scaling in chemical reactions at and away from equilibrium,” *J. Chem. Phys.* **157**, 194105 (2022).
 - [16] N. Goldenfeld, *Lectures on Phase Transitions and the Renormalization Group* (CRC Press, Boca Raton, 1992).
 - [17] U. C. Täuber, *Critical dynamics: a field theory approach to equilibrium and non-equilibrium scaling behavior* (Cambridge University Press, Cambridge, UK, 2014).
 - [18] G. Grinstein, “Generic scale invariance in classical nonequilibrium systems (invited),” *J. Appl. Phys.* **69**, 5441 (1991).
 - [19] G. Grinstein, “Generic scale invariance and self-organized criticality,” in *Scale Invariance, Interfaces and Nonequilibrium Dynamics*, edited by A. McKane, M. Droz, J. Vannimenus, and D. Wolf (Plenum, New York, 1995) p. 261.
 - [20] D. Belitz, T. R. Kirkpatrick, and T. Vojta, “How generic scale invariance influences phase transitions,” *Rev. Mod. Phys.* **77**, 579 (2005).
 - [21] M. Kardar, G. Parisi, and Y.-C. Zhang, “Dynamic scaling of growing interfaces,” *Phys. Rev. Lett.* **56**, 889 (1986).
 - [22] T. Kriecherbauer and J. Krug, “A pedestrian’s view on interacting particle systems, KPZ universality and random matrices,” *J. Phys. A: Math. Theor.* **43**, 403001 (2010).
 - [23] K. A. Takeuchi, “An appetizer to modern developments on the Kardar–Parisi–Zhang universality class,” *Physica A* **504**, 77 (2018).
 - [24] L. Chen, C. F. Lee, and J. Toner, “Mapping two-dimensional polar active fluids to two-dimensional soap and one-dimensional sandblasting,” *Nat. Commun.* **7**, 12215 (2016).
 - [25] D. Wei, A. Rubio-Abadal, B. Ye, F. Machado, J. Kemp, K. Srakaew, S. Hollerith, J. Rui, S. Gopalakrishnan, N. Y. Yao, I. Bloch, and J. Zeiher, “Quantum gas microscopy of Kardar-Parisi-Zhang superdiffusion,” *Science* **376**, 716 (2022).
 - [26] Q. Fontaine, D. Squizzato, F. Baboux, I. Amelio, A. Lemaître, M. Morassi, I. Sagnes, L. Le Gratiet, A. Harouri, M. Wouters, I. Carusotto, A. Amo, M. Richard, A. Minguzzi, L. Canet, S. Ravets, and J. Bloch, “Kardar-Parisi-Zhang universality in a one-dimensional polariton condensate,” *Nature* **608**, 687 (2022).
 - [27] C. A. Tracy and H. Widom, “The Distributions of Random Matrix Theory and their Applications,” *New Trends Math. Phys.* **0553379**, 753 (2009).
 - [28] J.-Y. Fortin and M. Clusel, “Applications of Extreme Value Statistics,” *J. Phys. A: Math. Theor.* **48**, 183001 (2015).
 - [29] G. Makey, S. Galioglu, R. Ghaffari, E. D. Engin, G. Yıldırım, Ö. Yavuz, O. Bektaş, Ü. S. Nizam, Ö. Akbulut, Ö. Şahin, K. Güngör, D. Dede, H. V. Demir, F. Ö. Ilday, and S. Ilday, “Universality of dissipative self-assembly from quantum dots to human cells,” *Nature Phys.* **16**, 795 (2020).
 - [30] H. Sakaguchi, S. Shinomoto, and Y. Kuramoto, “Mutual Entrainment in Oscillator Lattices with Nonvariational Type Interaction,” *Prog. Theor. Phys.* **79**, 1069 (1988).
 - [31] G. Grinstein, D. Mukamel, R. Seidin, and C. H. Bennett, “Temporally periodic phases and kinetic roughen-

- ing,” *Phys. Rev. Lett.* **70**, 3607 (1993).
- [32] H. Chaté and P. Manneville, “Phase diagram of the two-dimensional complex Ginzburg-Landau equation,” *Physica A (Amsterdam)* **224**, 348–368 (1996).
- [33] P. Manneville and H. Chaté, “Phase turbulence in the two-dimensional complex Ginzburg-Landau equation,” *Physica D* **96**, 30–46 (1996).
- [34] R. Gutiérrez and R. Cuerno, “Nonequilibrium criticality driven by Kardar-Parisi-Zhang fluctuations in the synchronization of oscillator lattices,” *Phys. Rev. Research* **5**, 023047 (2023).
- [35] J. A. Acebrón, L. L. Bonilla, C. J. Pérez Vicente, F. Ritort, and R. Spigler, “The Kuramoto model: A simple paradigm for synchronization phenomena,” *Rev. Mod. Phys.* **77**, 137 (2005).
- [36] V. H. Purrello, J. L. Iguain, and A. B. Kolton, “Roughening of the anharmonic Larkin model,” *Phys. Rev. E* **99**, 032105 (2019).
- [37] I. G. Szendro, J. M. López, and M. A. Rodríguez, “Localization in disordered media, anomalous roughening, and coarsening dynamics of faceted surfaces,” *Phys. Rev. E* **76**, 011603 (2007).
- [38] S. H. Strogatz, *Nonlinear Dynamics and Chaos: With Applications to Physics, Biology, Chemistry, and Engineering, 2nd Ed.* (CRC Press, Boca Raton, FL, 2015).
- [39] B. Pietras and A. Daffertshofer, “Network dynamics of coupled oscillators and phase reduction techniques,” *Phys. Rep.* **819**, 1 (2019).
- [40] See the Supplemental Material at ... for a phase-reduction study of rings of SL and vdP oscillators, numerical results concerning real-space correlations and phase trajectories, and details on phase extraction in the vdP case.
- [41] R. Lauter, A. Mitra, and F. Marquardt, “From Kardar-Parisi-Zhang scaling to explosive desynchronization in arrays of limit-cycle oscillators,” *Phys. Rev. E* **96**, 012220 (2017).
- [42] J. P. Moroney and P. R. Eastham, “Synchronization in disordered oscillator lattices: Nonequilibrium phase transition for driven-dissipative bosons,” *Phys. Rev. Research* **3**, 043092 (2021).
- [43] H. Nakao, “Phase reduction approach to synchronisation of nonlinear oscillators,” *Contemp. Phys.* **57**, 188 (2016).
- [44] V. García-Morales and K. Krischer, “The complex Ginzburg-Landau equation: an introduction,” *Contemp. Phys.* **53**, 79 (2012).
- [45] M. Siegert, “Determining exponents in models of kinetic surface roughening,” *Phys. Rev. E* **53**, 3209 (1996).
- [46] J. M. López, M. A. Rodríguez, and R. Cuerno, “Power spectrum scaling in anomalous kinetic roughening of surfaces,” *Physica A* **246**, 329 (1997).
- [47] J. J. Ramasco, J. M. López, and M. A. Rodríguez, “Generic dynamic scaling in kinetic roughening,” *Phys. Rev. Lett.* **84**, 2199 (2000).
- [48] F. Family and T. Vicsek, “Scaling of the active zone in the eden process on percolation networks and the ballistic deposition model,” *J. Phys. A: Math. Gen.* **18**, L75 (1985).
- [49] The errors in the exponent values can be considered smaller than 0.05; the exponent values must be adjusted quite precisely in order to satisfy the scaling constraints of $W(L, t)$, $S(k, t)$ and $G(r, t)$.
- [50] M. Schroeder and M. Siegert, “Scaling of growing surfaces with large local slopes,” *Europhys. Lett.* **24**, 563 (1993).
- [51] S. Das Sarma, S. V. Ghaisas, and J. M. Kim, “Kinetic super-roughening and anomalous dynamic scaling in nonequilibrium growth models,” *Phys. Rev. E* **49**, 122 (1994).
- [52] J. M. López, M. A. Rodríguez, and R. Cuerno, “Superroughening versus intrinsic anomalous scaling of surfaces,” *Phys. Rev. E* **56**, 3993 (1997).
- [53] R. Cuerno and L. Vázquez, “Universality issues in surface kinetic roughening of thin solid films,” in *Advances in Condensed Matter and Statistical Physics*, edited by E. Korutcheva and R. Cuerno (Nova Science Publishers, New York, 2004).
- [54] B. G. Barreales, J. J. Meléndez, R. Cuerno, and J. J. Ruiz-Lorenzo, “Kardar-Parisi-Zhang universality class for the critical dynamics of reaction-diffusion fronts,” *J. Stat. Mech.* **2020**, 023203 (2020).
- [55] C. Misbah, *Complex Dynamics and Morphogenesis: An Introduction to Nonlinear Science* (Springer, Dordrecht, Netherlands, 2016).
- [56] R. H. Rand and P. J. Holmes, “Bifurcation of periodic motions in two weakly coupled van der Pol oscillators,” *Int. J. Non-Linear Mech.* **15**, 387 (1980).
- [57] T. Nattermann and W. Renz, “Diffusion in a random catalytic environment, polymers in random media, and stochastically growing interfaces,” *Phys. Rev. A* **40**, 4675 (1989).
- [58] J. Krug and T. Halpin-Healy, “Directed polymers in the presence of columnar disorder,” *J. Phys. I France* **3**, 2179 (1993).
- [59] M. Itoh, “Synthesis of electronic circuits for simulating nonlinear dynamics,” *Int. J. Bif. Chaos* **11**, 605 (2001).
- [60] B. Choubey, “An experimental investigation of coupled van der Pol oscillators,” *J. Vib. Acoust.* **132**, 0310131 (2010).
- [61] H. Kori, Y. Kuramoto, S. Jain, I. Z. Kiss, and J. L. Hudson, “Clustering in globally coupled oscillators near a Hopf bifurcation: Theory and experiments,” *Phys. Rev. E* **89**, 062906 (2014).

SUPPLEMENTAL MATERIAL:

Kardar-Parisi-Zhang fluctuations in the synchronization dynamics of limit-cycle oscillators

PHASE REDUCTION OF A CHAIN OF STUART-LANDAU OSCILLATORS

The dynamics of a ring (i.e. a one-dimensional chain with periodic boundary conditions) comprising L diffusively-coupled Stuart-Landau (SL) oscillators is given by

$$\dot{z}_j(t) = a_j z_j(t) - b_j |z_j(t)|^2 z_j(t) + K c_j [z_{j+1}(t) + z_{j-1}(t) - 2z_j(t)], \quad j = 1, 2, \dots, L, \quad (\text{S1})$$

where $z_{L+1} \equiv z_1$ and $z_0 \equiv z_L$. In the ensuing discussion we focus on a reference oscillator, for which we drop the subindex j , and replace z_{j+1} by z_r (right neighbor) and z_{j-1} by z_ℓ (left neighbor). Except for the (real) coupling strength K , all parameters are complex, so $a = a_R + ia_I$, $b = b_R + ib_I$ and $c = c_R + ic_I$, thus

$$\dot{z}(t) = (a_R + ia_I)z(t) - (b_R + ib_I)|z(t)|^2 z(t) + K(c_R + ic_I)[z_r(t) + z_\ell(t) - 2z(t)]. \quad (\text{S2})$$

In the absence of coupling, $K = 0$, the system has a limit cycle solution of radius $R_c = \sqrt{a_R/b_R}$, with intrinsic frequency $\omega = a_I - b_I a_R/b_R$, as it is easy to check by trying a solution of the form $z(t) = R(t)e^{i\phi(t)}$. For the parameter choices considered in the main text, $a = \mu + i\omega$, $b = 1$ and $c = 1 + i$, which yields a stable limit cycle of radius $\sqrt{\mu}$ with oscillation frequency $\omega = a_I$ (which changes from one oscillator to another).

It has been shown [39, 61] that the equation above can be reduced to a phase model for coupling $K = \mu\kappa$, of order $\mathcal{O}(\mu)$, when the trajectory of $z(t)$ deviates slightly from the unperturbed limit cycle. In such a case, the solution can thus be approximated by $z(t) \approx R(t)e^{i\phi(t)}$, where the phase $\phi(t)$ evolves according to

$$\dot{\phi} = \omega + \mu\kappa \mathbf{Z}(z^0) \cdot h(z^0, z_\ell^0, z_r^0). \quad (\text{S3})$$

Here, $\mathbf{Z}(z_0)$ is the so-called phase sensitivity function and $h(z^0, z_\ell^0, z_r^0)$ is the coupling function, which are evaluated on the limit cycle, and dot stands for the complex inner product [39, 61]. Both these functions can be written in terms of the phases [2, 61] as

$$\mathbf{Z}(\phi) = \frac{-b_I/b_R + i}{R_c} e^{i\phi}, \quad (\text{S4})$$

and

$$h(\phi^0, \phi_\ell^0, \phi_r^0) = \mu\kappa\gamma R_c [e^{i\phi_r} + e^{i\phi_\ell} - 2e^{i\phi}]. \quad (\text{S5})$$

By introducing these expressions into Eq. (S3) and averaging over a full period, we are finally left with a closed equation for the phases, namely

$$\dot{\phi} = \omega + \mu\kappa [\Gamma(\phi_r - \phi) + \Gamma(\phi_\ell - \phi)]. \quad (\text{S6})$$

The function $\Gamma(\psi)$ that couples phases to one another in Eq. (S6) can be expanded in a Fourier series, $\Gamma(\psi) = A_0 + \sum_{k=1}^{\infty} (A_k \cos k\psi + B_k \sin k\psi)$, which yields,

$$A_0 = -A_1 = \frac{c_R b_I}{b_R} - c_I, \quad (\text{S7})$$

$$B_1 = c_R + \frac{c_I b_I}{b_R}, \quad (\text{S8})$$

while all other coefficients vanish at this order of approximation. Again, for the parameters employed in the main text, we obtain $A_0 = -A_1 = -1$, and $B_1 = 1$, thus the coupling function is

$$\Gamma(\psi) = -1 + \cos \psi + \sin \psi. \quad (\text{S9})$$

As the coupling function is certainly not odd [$\Gamma(\psi) + \Gamma(-\psi) \neq 0$], the phase-reduced model should yield the KPZ equation with columnar noise in the continuum approximation according to the arguments given in Ref. [34]. This is compatible with the generic scale invariant (GSI) behavior observed in the numerical results of the main text. In fact, the phase-reduced dynamics with coupling given by Eq. (S9) corresponds to one of the parameter choices of the sinusoidal (Kuramoto-Sakaguchi) coupling thoroughly investigated in Ref. [34], namely $\delta = \pi/4$.

PHASE REDUCTION OF A CHAIN OF VAN DER POL OSCILLATORS

The dynamics of the ring of L diffusively-coupled van der Pol (vdP) oscillators considered in the main text is given by

$$\ddot{x}_j(t) = (\mu - x_j^2(t))\dot{x}_j(t) - \omega_j^2 x_j(t) + K[(x_{j+1}(t) + x_{j-1}(t) - 2x_j(t)) + (\dot{x}_{j+1}(t) + \dot{x}_{j-1}(t) - 2\dot{x}_j(t))], \quad j = 1, 2, \dots, L, \quad (\text{S10})$$

where $x_{L+1} \equiv x_1$ and $x_0 \equiv x_L$. We again focus our discussion on a single oscillator, whose state is given by x and $v \equiv \dot{x}$ (we omit the subscript for simplicity), while that of its left (right) neighbor is given by x_ℓ and $v_\ell \equiv \dot{x}_\ell$ (x_r and $v_r \equiv \dot{x}_r$). The dynamics of the reference oscillator can be expressed as a system of two ordinary differential equations in the standard manner,

$$\begin{pmatrix} \dot{x} \\ \dot{v} \end{pmatrix} = \begin{pmatrix} 0 & 1 \\ -\omega^2 & \mu \end{pmatrix} \begin{pmatrix} x \\ v \end{pmatrix} + \begin{pmatrix} 0 \\ -x^2 v \end{pmatrix} + K \left[\begin{pmatrix} 0 & 0 \\ -2 & -2 \end{pmatrix} \begin{pmatrix} x \\ v \end{pmatrix} + \begin{pmatrix} 0 & 0 \\ 1 & 1 \end{pmatrix} \begin{pmatrix} x_\ell \\ v_\ell \end{pmatrix} + \begin{pmatrix} 0 & 0 \\ 1 & 1 \end{pmatrix} \begin{pmatrix} x_r \\ v_r \end{pmatrix} \right]. \quad (\text{S11})$$

Following the usual assumptions of phase-reduction theory [2, 39], we consider that the coupling function and the differences between oscillators as given by the intrinsic frequencies are proportional to the parameter μ , which measures the distance of the vdP oscillator to its Hopf bifurcation. Thus, $K = \mu\kappa$ and $\omega = \bar{\omega} + \mu\Delta\omega$, where $\mu\Delta\omega$ accounts for the deviation in the intrinsic frequency of the reference oscillator ω from the average of the distribution of intrinsic frequencies in the chain, $\bar{\omega}$. We thus rewrite Eq. (S11) as

$$\begin{aligned} \begin{pmatrix} \dot{x} \\ \dot{v} \end{pmatrix} &= \begin{pmatrix} 0 & 1 \\ -\bar{\omega}^2 & 0 \end{pmatrix} \begin{pmatrix} x \\ v \end{pmatrix} + \mu \begin{pmatrix} 0 & 0 \\ 0 & 1 \end{pmatrix} \begin{pmatrix} x \\ v \end{pmatrix} + \begin{pmatrix} 0 \\ -x^2 v \end{pmatrix} \\ &+ \mu \begin{pmatrix} 0 & 0 \\ -2\bar{\omega}\Delta\omega & 0 \end{pmatrix} \begin{pmatrix} x \\ v \end{pmatrix} + \mu^2 \begin{pmatrix} 0 & 0 \\ -(\Delta\omega)^2 & 0 \end{pmatrix} \begin{pmatrix} x \\ v \end{pmatrix} + \mu\kappa \left[\begin{pmatrix} 0 & 0 \\ -2 & -2 \end{pmatrix} \begin{pmatrix} x \\ v \end{pmatrix} + \begin{pmatrix} 0 & 0 \\ 1 & 1 \end{pmatrix} \begin{pmatrix} x_\ell \\ v_\ell \end{pmatrix} + \begin{pmatrix} 0 & 0 \\ 1 & 1 \end{pmatrix} \begin{pmatrix} x_r \\ v_r \end{pmatrix} \right]. \end{aligned} \quad (\text{S12})$$

Adapting the notation in Ref. [39] to our discussion, the equation above can be seen as $\dot{\mathbf{x}} = \mathbf{f}(\mathbf{x}, \mu) + \mu\mathbf{g}(\mathbf{x}, \mathbf{x}_\ell, \mathbf{x}_r, \mu)$, where $\mathbf{f}(\mathbf{x}, \mu)$ gives the unperturbed dynamics (identical for each oscillator in the chain) in the first line on the right-hand side of Eq. (S12), while the second line corresponds to the perturbation $\mu\mathbf{g}(\mathbf{x}, \mathbf{x}_\ell, \mathbf{x}_r, \mu)$, which in our case contains both the coupling to the neighboring oscillators and the randomness in the distribution of intrinsic frequencies as given by $\mu\Delta\omega$. (See e.g. Ch. 5 of Ref. [2] for other examples where parameter mismatches are treated as a perturbation.) The unperturbed dynamics can be written as

$$\begin{aligned} \mathbf{f}(\mathbf{x}, t; \mu) &= \mathbf{L}_0 \mathbf{x} + \mu \mathbf{L}_1 \mathbf{x} + \mathbf{N}_0 \mathbf{x} \mathbf{x} \mathbf{x}, \\ \mathbf{L}_0 &= \begin{pmatrix} 0 & 1 \\ -\bar{\omega}^2 & 0 \end{pmatrix}, \quad \mathbf{L}_1 = \begin{pmatrix} 0 & 0 \\ 0 & 1 \end{pmatrix}, \quad \mathbf{N}_0 \mathbf{x} \mathbf{x} \mathbf{x} = \begin{pmatrix} 0 \\ -x^2 v \end{pmatrix}, \end{aligned} \quad (\text{S13})$$

where the nonlinear contribution corresponds to $\mathbf{N}_0 \mathbf{x} \mathbf{x} \mathbf{x} = \mathbf{n}_3(\mathbf{x}^{(1)}, \mathbf{x}^{(2)}, \mathbf{x}^{(3)}, \mu = 0)$, with

$$\mathbf{n}_3(\mathbf{x}^{(1)}, \mathbf{x}^{(2)}, \mathbf{x}^{(3)}, \mu) = \sum_{i_1, i_2, i_3=1}^2 \frac{1}{3!} \left(\frac{\partial^3 \mathbf{f}(\mathbf{x}, t; \mu)}{\partial x_{i_1}^{(1)} \partial x_{i_2}^{(2)} \partial x_{i_3}^{(3)}} \right)_{\mathbf{x}=\mathbf{0}} x_{i_1}^{(1)} x_{i_2}^{(2)} x_{i_3}^{(3)}, \quad (\text{S14})$$

which in our case, for $x_1 \equiv x$ and $x_2 \equiv v$, does not depend on μ anyway. The only nonzero third-order derivatives are indeed

$$\frac{\partial^3 \mathbf{f}(\mathbf{x}, t; \mu)}{\partial x_1^{(1)} \partial x_1^{(2)} \partial x_2^{(3)}} = \frac{\partial^3 \mathbf{f}(\mathbf{x}, t; \mu)}{\partial x_2^{(1)} \partial x_1^{(2)} \partial x_1^{(3)}} = \frac{\partial^3 \mathbf{f}(\mathbf{x}, t; \mu)}{\partial x_1^{(1)} \partial x_2^{(2)} \partial x_1^{(3)}} = -2. \quad (\text{S15})$$

Quadratic terms or terms of order higher than $\mathcal{O}(|\mathbf{x}|^3)$ do not appear in Eq. (S13), as they are absent from the vdP oscillator dynamics [see Eq. (S12), first line]. As for the perturbation $\mathbf{g}(\mathbf{x}, \mathbf{x}_\ell, \mathbf{x}_r, \mu)$, we just focus on the lowest-order terms in μ [which implies neglecting the term containing $(\Delta\omega)^2$ in the second line of Eq. (S12)]. As those terms are all linear in the state vectors of the reference oscillator and its neighbors, the expansion yields

$$\begin{aligned} \mathbf{g}(\mathbf{x}, \mathbf{x}_\ell, \mathbf{x}_r, \mu) &= G \mathbf{x} + G_\ell \mathbf{x}_\ell + G_r \mathbf{x}_r, \\ G &= \begin{pmatrix} 0 & 0 \\ -2\bar{\omega}\Delta\omega - 2\kappa & -2\kappa \end{pmatrix}, \quad G_\ell = G_r = \begin{pmatrix} 0 & 0 \\ \kappa & \kappa \end{pmatrix}. \end{aligned} \quad (\text{S16})$$

In the unperturbed dynamics at the bifurcation point, $\mu = 0$, the origin $x = \dot{x} = 0$ loses its stability. The linearized dynamics there is given by $\dot{\mathbf{x}} = \mathbf{L}_0 \mathbf{x}$, with eigenvalues $\lambda_{\pm} = \pm i\bar{\omega}$, right eigenvectors $\mathbf{u}_{\pm} = (1, \pm i\bar{\omega})^T$, and left eigenvectors $\mathbf{v}_{\pm} = (1/2, \mp i/2\bar{\omega})$, where the normalization has been chosen so that $\mathbf{v}_{\pm} \mathbf{u}_{\pm} = 1$. The solution of the linearized unperturbed system at $\mu = 0$ is thus given by

$$\mathbf{x}_0(t) = Z e^{i\bar{\omega}t} \mathbf{u}_+ + Z^* e^{-i\bar{\omega}t} \mathbf{u}_-. \quad (\text{S17})$$

where the so-called complex amplitude Z is just a constant. In the standard perturbative approach, the solution of the perturbed dynamics for $0 < \mu \ll 1$ is taken to have the same form, but with a time-dependent amplitude $Z(t)$, whose typical time scale is $\tau = \mu t$. By a time-scale separation procedure due to Y. Kuramoto (see Ref. [2], and also Ref. [39] for some other formulations giving analogous results), one can show that the complex amplitude at the lowest order of approximation is governed by the Stuart-Landau (SL) equation

$$\dot{Z}(t) = aZ(t) - b|Z(t)|^2 Z(t) + \mu[cZ(t) + c_{\ell}Z_{\ell}(t) + c_rZ_r(t)] \quad (\text{S18})$$

with parameters

$$a = \mu \mathbf{v}_+ \mathbf{L}_1 \mathbf{u}_+ = \mu (1/2, -i/2\bar{\omega}) \begin{pmatrix} 0 & 0 \\ 0 & 1 \end{pmatrix} \begin{pmatrix} 1 \\ i\bar{\omega} \end{pmatrix} = \frac{\mu}{2}, \quad (\text{S19})$$

$$b = -3\mathbf{v}_+ \mathbf{N}_0 \mathbf{u}_+ \mathbf{u}_+ \mathbf{u}_+^* = -3(1/2, -i/2\bar{\omega}) \begin{pmatrix} 0 \\ -\frac{2}{3!}(i\bar{\omega} + i\bar{\omega} - i\bar{\omega}) \end{pmatrix} = \frac{1}{2}, \quad (\text{S20})$$

$$c = \mathbf{v}_+ \mathbf{G} \mathbf{u}_+ = (1/2, -i/2\bar{\omega}) \begin{pmatrix} 0 & 0 \\ -2\bar{\omega}\Delta\omega - 2\kappa & -2\kappa \end{pmatrix} \begin{pmatrix} 1 \\ i\bar{\omega} \end{pmatrix} = -\kappa + i(\Delta\omega + \kappa/\bar{\omega}), \quad (\text{S21})$$

$$c_{\ell/r} = \mathbf{v}_+ \mathbf{G}_{\ell/r} \mathbf{u}_+ = (1/2, -i/2\bar{\omega}) \begin{pmatrix} 0 & 0 \\ \kappa & \kappa \end{pmatrix} \begin{pmatrix} 1 \\ i\bar{\omega} \end{pmatrix} = \frac{\kappa}{2} - i\frac{\kappa}{2\bar{\omega}}. \quad (\text{S22})$$

The SL equation that results is thus

$$\dot{Z}(t) = \mu \left(\frac{1}{2} + i\Delta\omega \right) Z(t) - \frac{1}{2} |Z(t)|^2 Z(t) + K \left(\frac{1}{2} - i\frac{1}{2\bar{\omega}} \right) [Z_{\ell}(t) + Z_r(t) - 2Z(t)], \quad (\text{S23})$$

where again $K = \mu\kappa$. The solution of the perturbed system is thus given by $\mathbf{x}(t) \approx Z(t)e^{i\bar{\omega}t} \mathbf{u} + \text{c.c.}$, with $Z(t)$ satisfying Eq. (S23), where c.c. denotes complex conjugation. In terms of $z(t) \equiv Z(t)e^{i\bar{\omega}t}$, the solution to lowest order in μ becomes $\mathbf{x}(t) \approx z(t)\mathbf{u} + \text{c.c.}$, with

$$\dot{z}(t) = \left(\frac{\mu}{2} + i \underbrace{(\bar{\omega} + \mu\Delta\omega)}_{\omega} \right) z(t) - \frac{1}{2} |z(t)|^2 z(t) + K \left(\frac{1}{2} - i\frac{1}{2\bar{\omega}} \right) [z_{\ell}(t) + z_r(t) - 2z(t)]. \quad (\text{S24})$$

In the particular case of uncoupled dynamics, $K = 0$, a solution to this equation is easily obtained in polar coordinates, yielding a (stable for $\mu > 0$) limit cycle of radius $\sqrt{\mu}$ with intrinsic frequency ω .

The vdP oscillator can thus be approximated (close to the bifurcation point) by a SL oscillator, Eq. (S2), with $a = \mu/2 + i\omega$, $b = 1/2$, and $c = 1/2 - i/2\bar{\omega}$. Therefore, as discussed in the previous section, the Fourier coefficients of the coupling function $\Gamma(\psi) = A_0 + \sum_{k=1}^{\infty} (A_k \cos k\psi + B_k \sin k\psi)$ which appears in the phase-reduced model are

$$A_0 = -A_1 = \frac{c_R b_I}{b_R} - c_I = \frac{1}{2\bar{\omega}}, \quad (\text{S25})$$

$$B_1 = c_R + \frac{c_I b_I}{b_R} = 1/2, \quad (\text{S26})$$

all the other vanishing at this order of approximation. Thus the coupling function is

$$\Gamma(\psi) = \frac{1}{2\bar{\omega}} (1 - \cos \psi) + \frac{1}{2} \sin \psi. \quad (\text{S27})$$

As this function is certainly not odd [$\Gamma(\psi) + \Gamma(-\psi) \neq 0$] hence the KPZ nonlinearity appears in the continuum approximation with columnar noise [34]. This is compatible with the generic scale invariant (GSI) behavior observed in the numerical results of the main text.

REAL-SPACE PHASE CORRELATIONS AND MORPHOLOGIES

The real-space two-point (phase-difference) correlations are defined as

$$G(r, t) = \overline{\langle (\phi_{j+r}(t) - \phi_j(t))^2 \rangle}, \quad (\text{S28})$$

with the overbar denoting spatial average across the oscillator ring and the brackets denoting average over different disorder (i.e. intrinsic frequency) realizations. Due to invariance under reversal $r \rightarrow -r$, the correlations only depend on $\ell \equiv |r|$. We will be interested in cases such that $\alpha_s > 1$, for which the correlation function scales as [46]

$$G(\ell, t) \sim \begin{cases} t^{2\beta}, & \text{if } t^{1/z} \ll \ell \ll L, \\ \ell^{2\alpha_{\text{loc}}} t^{2(\alpha - \alpha_{\text{loc}})/z}, & \text{if } \ell \ll t^{1/z} \ll L. \end{cases} \quad (\text{S29})$$

This means that the two-point correlations keep increasing (anomalously) with time even at distances which are smaller than the correlation length, as they only saturate at $\ell^{2\alpha_{\text{loc}}} L^{2(\alpha - \alpha_{\text{loc}})}$ when $t^{1/z} \sim L$. If $\alpha \neq \alpha_s$ with both exponents being larger than 1, as in our case, faceted anomalous scaling takes place [47], and $\alpha_{\text{loc}} = 1$.

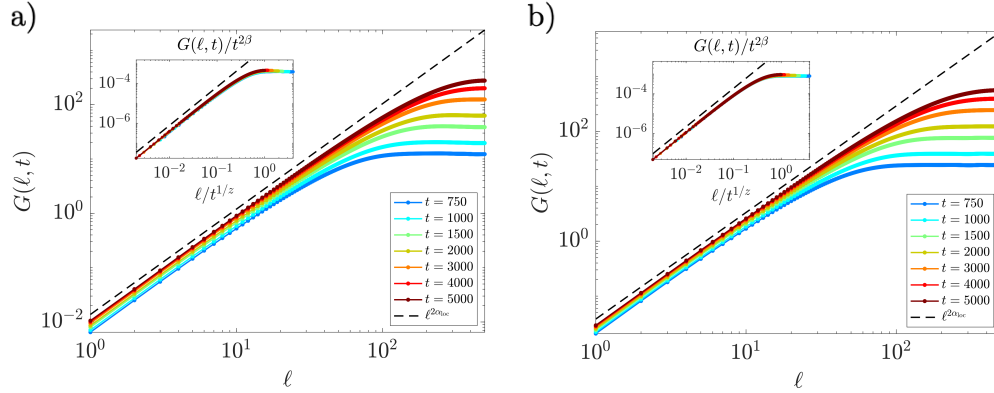


FIG. S4. Two-point correlations for rings of (a) SL and (b) vdP oscillators with (inset) and without (main panel) rescaling as given by Eq. (S29). Results shown for $\mu = 1$, $L = 1000$, and 1000 realizations. Exponent values: $\alpha = 1.07$, $z = 1.37$ and $\alpha_{\text{loc}} = 0.97$ ($\beta = \alpha/z \approx 0.78$).

The correlations, Eq. (S28), for a ring of SL oscillators are displayed in Fig. S4 (a), while analogous results are shown in panel (b) for vdP oscillators. In both cases we have chosen $\mu = 1$. While the values of the exponents α , α_s , and z are those of the main text (see caption), and $\beta = \alpha/z$, the value of the local roughness exponent, namely $\alpha_{\text{loc}} = 0.97$, has been obtained from the results here displayed, as well as similar ones obtained for other values of μ (not shown). The small discrepancy of this value with respect to the theoretically expected value may well be a finite-size effect. In the inset, the rescaled form $G(\ell, t)/t^{2\beta}$ is shown as a function of the rescaled length $\ell/t^{1/z}$, which confirms the anomalous increase mentioned above as well as the growth $G(\ell, t) \sim \ell^{2\alpha_{\text{loc}}}$ for lengths smaller than the correlation length.

We next illustrate the morphologies of the phase profiles in the trajectories of the rings of oscillators under consideration. Two representative trajectories are displayed in Fig. S5, for a ring of SL oscillators in panel (a), and for a ring of vdP oscillators in panel (b), both corresponding again to $\mu = 1$. Triangular facets are quite conspicuous throughout the synchronization process. They display the same characteristic coarsening dynamics previously observed in phase oscillators [34, 42] as well as in the height profile of the KPZ equation with columnar noise [37].

DYNAMICAL PHASE FOR RINGS OF VDP OSCILLATORS

As noted in the main text, even in the absence of nearest-neighbor coupling, a single vdP oscillator $(x_j(t), \dot{x}_j(t))$ behaves more and more as a relaxation oscillator for increasing values of μ , moving across different regions on the limit cycle (which differs very strongly from a circle, see Fig. 1 of the main text, in which $\mu = 1$) at different speeds [38]. Thus, the geometric phase given by $\arctan(\dot{x}_j/x_j)$ (taking into account the quadrant) no longer behaves as a valid dynamical phase variable [1]. Due to the lack of an analytical expression for the isochrones (as far as we are aware), in this case we define the phase by means of a Poincaré section [1]. We might set it at the half line given by

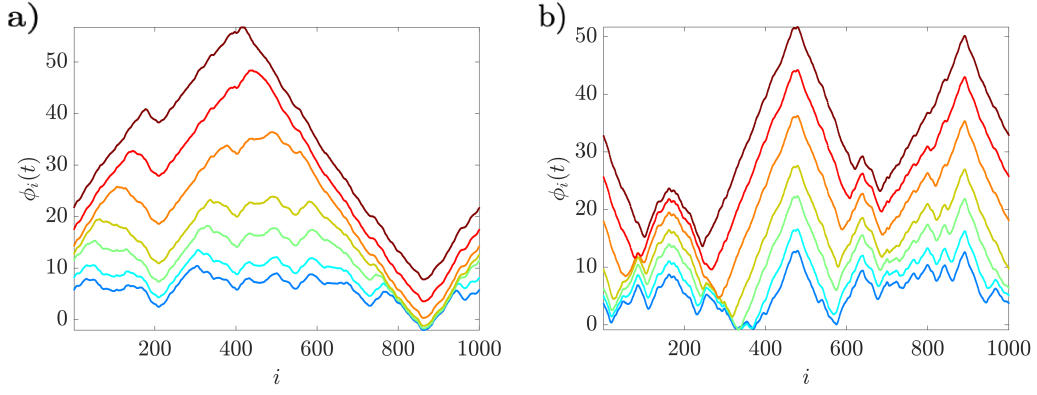


FIG. S5. Representative phase profiles across time for a ring of (a) SL and (b) vdP oscillators. Results shown for $\mu = 1$ and $L = 1000$. Color code as in Fig. S4. An arbitrary vertical displacement has been applied for visibility purposes.

$x_j > 0$ and $\dot{x}_j = 0$ in the phase portrait of oscillator j , so that, as \dot{x}_j goes from positive to negative for positive x_j , the phase ϕ_j increases by 2π with respect to the previous crossing of the section. In point of fact, that is what we would do in the absence of coupling ($K = 0$), but additional precautions need to be taken to avoid detecting spurious return times due to the ‘kicks’ received through the coupling with neighboring oscillators for $K > 0$. Specifically, two additional measures are adopted:

- i) we focus on sign changes of \dot{x}_j for $x_j > \sqrt{\mu}/5$, rather than just $x_j > 0$, to ensure that the oscillator goes across the ‘right’ part of the limit cycle by the time the Poincaré section is crossed —this allows for relatively strong effects due to coupling, as the limit cycle intersects the positive- x semiaxis at $(x_P, 0)$ for $x_P \approx \sqrt{\mu}$ for all μ under consideration;
- ii) we only record return times for which the time elapsed since the previous one is at least one tenth of the intrinsic period $2\pi/\omega_j$, so that no rapid back-and-forth oscillation across the section may be taken for a full period.

While no set of criteria along these lines is guaranteed to work under all imaginable circumstances, we have found that the results are robust against moderate variations on our choices. Thus, a set of phase trajectories $\{\phi_j(t)\}_{j=1}^L$ are obtained from the simulations of rings of vdP oscillators, which can then be used for computing the observables described in the main text, as well as in the previous section.